BIOCHEMISTRY
including biophysical chemistry & molecular biology

Article

pubs.acs.org/biochemistry

Bacterial Proteasome and PafA, the Pup Ligase, Interact to Form a Modular Protein Tagging and Degradation Machine

Nadav Forer,[†] Maayan Korman,[†] Yifat Elharar,[†] Marina Vishkautzan,[†,‡] and Eyal Gur*[,†,‡]

[†]Department of Life Sciences and [‡]The National Institute for Biotechnology in the Negev, Ben-Gurion University of the Negev, Beer-Sheva 84105, Israel

ABSTRACT: Proteasome-containing bacteria possess a tagging system that directs proteins to proteasomal degradation by conjugating them to a prokaryotic ubiquitin-like protein (Pup). A single ligating enzyme, PafA, is responsible for Pup conjugation to lysine side chains of protein substrates. As Pup is recognized by the regulatory subunit of the proteasome, Pup functions as a degradation tag. Pup presents overlapping regions for binding of the proteasome and PafA. It was, therefore, unclear whether Pup binding by the proteasome regulatory subunit, Mpa, and by PafA are mutually exclusive events. The work presented here provides evidence for the simultaneous interaction of Pup with both Mpa and PafA. Surprisingly, we found that PafA and Mpa can form a complex both *in vitro* and *in vivo*. Our results thus suggest that PafA and the proteasome can function as a modular machine for the tagging and degradation of cytoplasmic proteins.

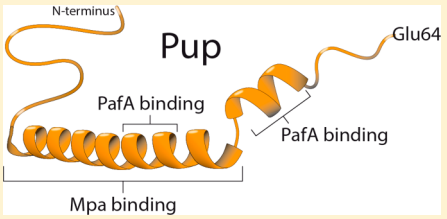

Bacteria belonging to the phyla Actinobacteria and Nitrospira possess proteasomes and a tagging system that directs proteins to proteasomal degradation.[1,2] While this degradation pathway is essential for full virulence of *Mycobacterium tuberculosis* (an actinobacteria), its role in nonpathogenic species has yet to be determined.[2−5] Bacterial proteasomes comprise homoheptameric α and β rings and are thus simpler than their eukaryotic counterparts, which contain heteroheptameric α and β rings.[6,7] Furthermore, the regulatory subunit of the bacterial proteasome is made up solely by a homohexameric AAA+ protein.[8,9] In most actinobacterial species, the regulatory subunit is termed ARC (AAA+ ATPase-forming ring-shaped complex),[10] whereas the mycobacterial ortholog is termed Mpa (mycobacterium proteasome ATPase).[8] Proteins are targeted to bacterial proteasomes following their conjugation to Pup, an intrinsically unstructured 64 amino acid protein.[11,12] The conjugation reaction is catalyzed by PafA (proteasome accessory factor A), an enzyme that forms an isopeptide bond between the γ-carboxylate of a glutamate at the C-terminus of Pup and the ε-amine of a substrate lysine.[11,13] In most actinobacterial species, Pup is translated with a glutamine, rather than a glutamate, at its C-terminus. A deamidation step, catalyzed by Dop (deamidase of Pup), converts this glutamine into a glutamate, thus preparing Pup for PafA-mediated conjugation (i.e., pupylation).[14] In a process called depupylation, Dop can also reverse the pupylation reaction by detaching an already conjugated Pup from pupylated substrates.[15,16]

Pupylated substrates can be degraded by the proteasome, as Pup functions as a degradation tag.[11,17] Specifically, it was shown in the *M. tuberculosis* system that the coiled coil N-terminal domain of Mpa interacts with a Pup region spanning residues 21−51, such that the Mpa domain acts to stabilize a helical conformation of this Pup region.[18] The N-terminal region of Pup enters the Mpa pore, thus promoting translocation of Pup, together with the conjugated substrate, into the 20S proteolytic chamber.[17,18] The C-terminal 26 residues of Pup correspond to the minimal Pup region necessary for PafA binding and conjugation to target substrates. The PafA−Pup interaction stabilizes helical conformations of Pup residues 38−47 and 51−58.[19] As such, the Pup regions involved in Mpa- and PafA-binding share an overlap of 19 residues[28−31] (Figure 1A). Based on Pup crystal structure analyses, several side chains within the overlapping region are involved in both PafA and Mpa binding.[18,19] For instance, Pup residues Leu39, Ile41, Leu46, and Leu47 contribute to Mpa binding by generating hydrophobic interactions with corresponding side chains of a Mpa coiled coil domain. The same Pup residues dock into a conserved PafA hydrophobic pocket. It is, therefore, possible that Mpa and PafA compete for Pup binding. In this study, this hypothesis was tested experimentally using purified recombinant *Mycobacterium smegmatis* proteins. We report that, in contrast to the expected, PafA and Mpa can bind Pup simultaneously. Furthermore, our experiments indicate that PafA and Mpa interact to form a complex and that this interaction differs from the interaction of PafA with its substrates. We suggest that despite the mutually exclusive binding of the Pup region between residues 38−47, PafA and Mpa can bind Pup simultaneously by formation of a ternary complex that is driven by an interaction between PafA and Mpa.

EXPERIMENTAL PROCEDURES

Expression and Purification of *M. smegmatis* Proteins.

Recombinant *M. smegmatis* proteins were used in this study.

Received: July 28, 2013
Revised: November 9, 2013
Published: November 14, 2013

   dx.doi.org/10.1021/bi401017b | *Biochemistry* 2013, 52, 9029−9035

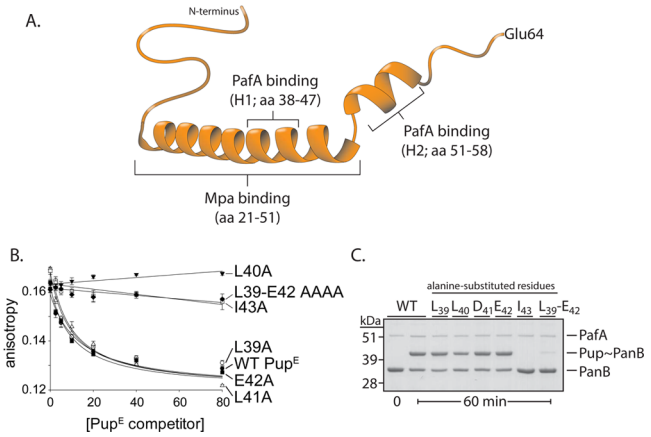

Figure 1. Pup^E presents overlapping PafA- and Mpa-binding regions. (A) A cartoon illustration of Pup^E depicting the regions involved in PafA and Mpa binding. (B) Fl-Pup^E (50 nM) anisotropy was measured in the presence of Mpa (0.67 μM hexamer) and increasing concentrations of the indicated Pup^E variants. The averages ± SD of three experiments are presented. The data obtained for the wild type, L39A, L41A and E42A Pup^E variants was fitted to a competitive inhibition model ($r = r_{max}$[Fl-Pup^E]/(K_D(1+[competitor]/$K_{0.5}$) + [Fl-Pup^E]), where r is the fluorescence anisotropy. The remaining curves were fitted to a linear regression. (C) SDS-PAGE analysis of the pupylation of PanB (5 μM) by PafA (1 μM) and the indicated Pup^E variants (10 μM each) is shown.

PafA and Pup variants were purified as described.[20] For Dop purification, *dop* was cloned into plasmid pSH21 containing a 5′ polyhistidine-coding sequence under the transcriptional control of the T7 promoter. Expression in *E. coli* was attained upon overnight growth at 16 °C. A standard Ni^{2+}-NTA purification protocol was followed for protein purification, with the exception that all buffers used contained 10% glycerol (v/v).

Mpa and Mpa^{KR} were expressed from plasmid pET11a in *E. coli* cells grown at 37 °C. After harvesting, cell pellets were resuspended in buffer A (25 mM Tris-HCl, pH 8.0, 10 mM $MgCl_2$, 1 mM DTT). Following cell lysis and centrifugation (15 000 *g*, 30 min), streptomycin sulfate (1% w/v) was added to the clear lysate for a 30 min incubation period. Centrifugation performed as above followed, after which the supernatant was filtered (0.22 μm) and loaded on a HiLoad QFF anionic exchange column equilibrated with buffer A. Elution was performed with a NaCl gradient (0−1 M) and Mpa-rich fractions were pooled and concentrated using Amicon concentrating units (Millipore). The concentrated protein solution was then loaded on a Superose6 column pre-equilibrated with buffer A. As a last purification step, a MonoQ column was employed with buffer A, with elution being carried out by a 0.1−0.8 M NaCl gradient. The purest fractions were pooled and a buffer exchange step was carried out using a PD10 column pre-equilibrated with buffer A. Mpa aliquots were prepared and kept at −80 °C.

For Fl-Mpa^{KR} purification, Mpa^{KR} bearing a C-terminal polyhistidine tag was expressed in *E. coli* cells grown at 37 °C. Following harvesting, the cell pellet was resuspended in buffer A containing 20 mM imidazole. Clear cell lysates were loaded onto a Ni^{2+}-NTA column pre-equilibrated with the same buffer, and after washing of unbound proteins, a buffer A-containing saturating concentration of 5-IAF was added. Following a 2 h incubation, bound labeled protein was washed with buffer A and elution was performed with buffer A containing 250 mM imidazole. As a second purification step, the protein was loaded on a gel filtration column (Superdex200), pre-equilibrated with buffer A containing 0.5 M NaCl.

Activity Assays. For ATPase measurements, NADH (1 mM) and LDH (10 U/mL) were added to the degradation buffer and assays were performed as described.[21,22] Quantitative pupylation assays were performed as described.[20] Fluorescence anisotropy binding measurements were performed in 384-well plates (50 μL reactions) using a Synergy2 plate reader (BioTek).

Pull-Down. Ni^{2+}-NTA agarose beads (50 μL) were transferred into filter microcentrifuge tubes (Corning ZQ-VW-8169) and washed three times by centrifugation (2 min, 4000 *g*) with 500 μL of 0.5 M EDTA to strip the beads from the associated nickel ions. Next, the stripped beads were washed three times with pupylation buffer (50 mM Tris-HCl pH 7.5, 100 mM KCl, 20 mM $MgCl_2$, and 10% glycerol (v/v)) and protein solutions were added to the beads (50 μL to each tube). Following a 5 min incubation, the protein-bound beads were washed three times with pupylation buffer. For elution, buffer (50 μL) containing 25 mM Tris-HCl, pH 8.0, and 0.5 M NaCl was used.

Co-Immunoprecipitation. A *pafA* gene carrying a 5′ FLAG coding sequence was cloned into plasmid pJV53[23] under the transcriptional control of an acetamide-induced mycobacterial promoter. The cloned plasmid was transformed into *M. smegmatis* strain MC^2155 and a liquid culture was grown at 37 °C in 7H9 growth medium containing kanamycin (10 mg/L). After the culture reached an $O.D._{600}$ of 0.5, it was incubated for 24 h and acetamide (0.2% (w/v)) was added to realize a 24 h window of FLAG-PafA induction. Cells were harvested, resuspended in PBS, disrupted by sonication, and the crude lysate was centrifuged for removal of cell debris. Next, 50 μL of the clear lysate and 2 μL of antibodies against Mpa, PafA, the 20S α subunit, or Dop were added to 950 μL PBS. Following a 1 h incubation, 35 μL of PBS-washed protein A sepharose beads were added for an additional hour. The suspension was centrifuged (2 min, 4000 *g*) and the beads were washed three times with PBS before desiccation by a speed vacuum centrifuge and resuspension in 100 μL protein-loading buffer.

RESULTS

As a first step in this study, we experimentally tested whether certain Pup residues are essential for both Mpa and PafA binding. Based on the available crystal structures of PafA and Mpa in complex with Pup,[18,19] we cloned and purified four Pup-glutamate (i.e., the C-terminally processed form of Pup, hereafter termed Pup^E) mutants harboring alanine substitutions of Leu39, Leu40, Asp41, Glu42, and Ile43. In addition, a mutant presenting a tetra-alanine substitution of Leu39-Glu42 was cloned and purified. To assess the effects of these mutations on Mpa binding, competition assays were performed in which Pup^E binding to Mpa was measured in the presence of increasing concentrations of mutant Pup^E competitors. Specifically, the ability of each mutant to compete with a N-terminally fluorescein-labeled Pup^E (Fl-Pup^E) for Mpa binding was determined by fluorescence anisotropy. We found that whereas Pup^E efficiently competes with Fl-Pup^E for Mpa Binding, the L40, I43, and the L39-E42 alanine substitution mutants do not (Figure 1B). In parallel, the interaction of Pup mutants with PafA was assessed by pupylation assays *in vitro*, using PanB as a target substrate. Poor conjugation of the tetra-

dx.doi.org/10.1021/bi401017b | *Biochemistry* 2013, 52, 9029−9035

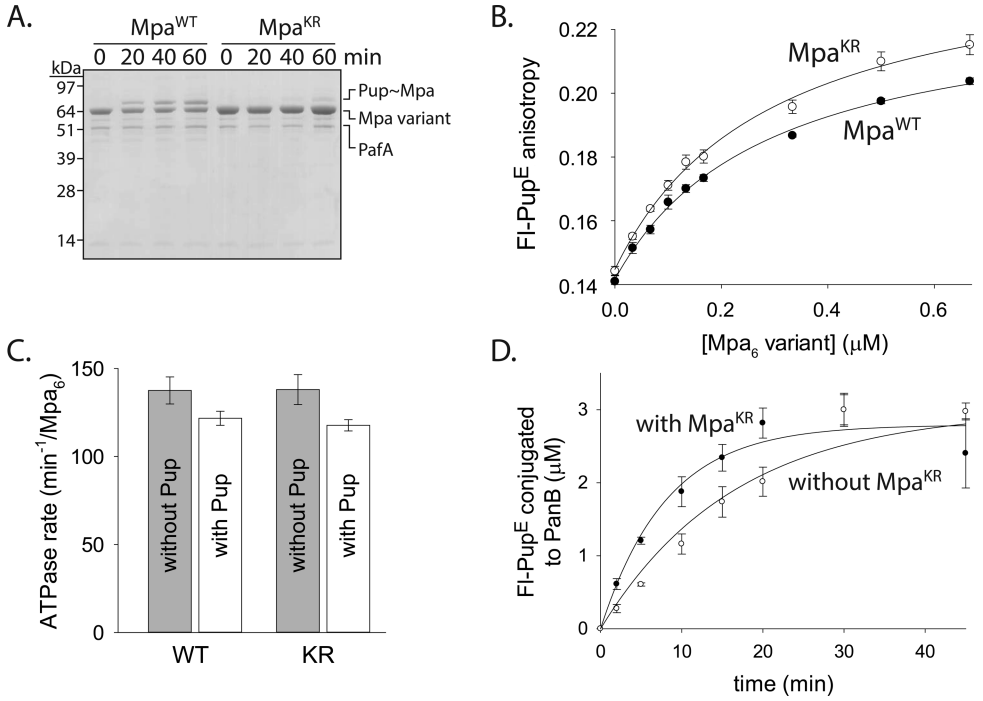

Figure 2. PafA and Mpa do not compete for Pup^E binding. (A) SDS-PAGE analysis of the pupylation of Mpa and Mpa^{KR} (0.5 μM hexamer each) by PafA (0.5 μM) and Pup^E (10 μM). (B) Fl-Pup^E (50 nM) anisotropy was measured at increasing concentrations of Mpa or Mpa^{KR}, as indicated. The curves are fitted to the binding equation $r = r_0 + (r_{max}[M])/(K_D + [M])$, where r is the fluorescence anisotropy value and M is either Mpa or Mpa^{KR}. (C) The rate of ATP hydrolysis by Mpa and Mpa^{KR} (0.3 μM hexamer each) was measured in the absence or presence of Pup^E (20 μM). (D) Pupylation of PanB (3 μM) by PafA (0.5 μM) and Fl-Pup^E (10 μM) in the absence or presence of Mpa^{KR} (10 μM hexamer). The curves are fitted to a single-exponential function. In all graphs, the average ± SD of three experiments are presented.

alanine substitution mutant (L39-E42) was observed (Figure 1C), whereas single alanine substitutions for Leu39, Leu40, Asp41, or Glu42 did not cause a detectable effect. By contrast, a single alanine substitution of Ile43 dramatically reduced PanB pupylation (Figure 1C), indicating a critical role for this residue in PafA binding. As Pup Ile43 is also essential for Mpa binding (Figure 1B), we surmise that binding of Pup helix H1 by Mpa and PafA is a mutually exclusive event.

The above data may suggest that Mpa and PafA compete for Pup binding. To experimentally test this hypothesis, we measured the kinetics of pupylation in the presence and in the absence of Mpa *in vitro*. If PafA and Mpa indeed compete for Pup binding, then under limiting Pup concentrations, a lower pupylation rate is expected in the presence of Mpa. However, analysis of such an experiment is potentially complicated as Mpa is a PafA pupylation substrate.[24−27] Therefore, to simplify our experimental system, we cloned and purified a Mpa pupylation-site mutant. In *M. tuberculosis* Mpa, lysine residue 591 constitutes a PafA pupylation site.[24,27] Sequence alignment analysis identified *M. smegmatis* Mpa lysine residue 595 to be a pupylation site. Indeed, a *M. smegmatis* Mpa K595R mutant (hereafter, Mpa^{KR}) was poorly pupylated by PafA, whereas an obvious pupylation product was detected when wild type Mpa served as substrate (Figure 2A). To test whether Mpa^{KR} binds Pup equally as well as the wild type protein, fluorescence anisotropy-based binding assays were carried out at increasing concentrations of each Mpa variant and at a constant concentration of Fl-Pup^E (Figure 2B). Thus, in a buffer used for pupylation assays, both Mpa and Mpa^{KR} bound Fl-Pup^E with a K_D of 0.29 ± 0.03 μM, indicating that the K595R mutation does not affect the Pup-binding ability of Mpa. The slightly higher anisotropy observed for Fl-Pup^E binding by Mpa^{KR} may result from a somewhat lower segmental mobility of the dye upon binding. The ATP hydrolysis rate of both Mpa variants was similar either in the presence or in the absence of Pup^E (Figure 2C). Together, these results suggest that the K595R mutation prevents efficient pupylation of Mpa by PafA, but otherwise does not affect the structural or catalytic properties of Mpa.

Next, pupylation rates of PanB, a model PafA substrate, were measured at a low PafA concentration (0.5 μM) in the absence and presence of Mpa^{KR}. Using 3 μM Fl-Pup^E, we calculated that 10 μM Mpa hexamers are sufficient to ensure that more than 85% of the Fl-Pup^E molecules are bound by Mpa, based on a K_D of 0.29 μM for Mpa^{KR}−Pup interaction, as measured in the experiment presented in Figure 2B. Under these conditions, if PafA and Mpa^{KR} compete for Fl-Pup^E binding, then PanB pupylation ought to be diminished, since PafA and Mpa present comparable affinities for Fl-Pup^E binding (Figure 2B and ref 20). However, no negative effect of Mpa^{KR} on pupylation was observed (Figure 2D). If any, a slight enhancement of PanB pupylation by PafA was noted. To better assess an effect of Mpa^{KR} on pupylation, PanB pupylation was measured under conditions in which PafA was saturated with either Fl-Pup^E or PanB. These experiments were carried our either in the presence or in the absence of Mpa^{KR}. While no effect on pupylation was observed when PafA was saturated with PanB, Mpa^{KR} stimulated pupylation 2-fold faster when PafA was saturated with Fl-Pup^E (Figure 3A). Measuring pupylation at under-saturating PanB concentrations and increasing Mpa^{KR} concentrations resulted in a hyperbolic curve that could be fitted to a rate equation with a K_{app} of 0.3 ± 0.15 μM for Mpa^{KR} activation (Figure 3B). These results suggest that Mpa and PafA can bind Pup^E simultaneously and that this interaction

dx.doi.org/10.1021/bi401017b | *Biochemistry* 2013, 52, 9029−9035

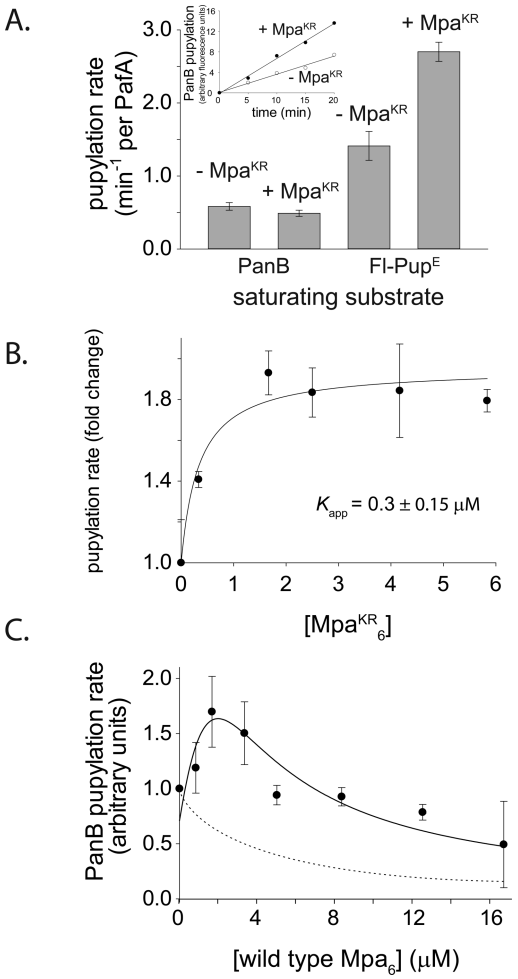

Figure 3. Effect of Mpa^{KR} on pupylation. (A) Pupylation reactions using 250 μM PanB with 0.5 μM Fl-Pup^{E} (left bars) and 25 mM PanB with 10 μM Fl-Pup^{E} (right bars). When added, Mpa^{KR} hexamers were used at a concentration of 8 μM. 0.17 μM PafA was used in all reactions. The averages ± SD of four experiments are presented. Pupylation at under-saturating PanB concentrations are shown in the inset. (B) PanB (50 μM) pupylation by PafA (0.17 μM) and Fl-Pup^{E} (1 μM) was measured at increasing concentrations Mpa^{KR}, as indicated. The curves are fitted to the rate equation $v = v_0 + (v_{max}[M])/(K_D + [M])$, where v is the pupylation rate and M is Mpa^{KR}. (C) Pupylation of PanB (1 μM) by PafA (0.5 μM) and Fl-Pup^{E} (10 μM) was measured at increasing concentrations of Mpa. The smooth curve was generated by fitting the data to the equation rate = $C\alpha(1 + \alpha + \beta)/(L + (1 + \alpha + \beta)^2)$, where C is a scaling factor, $\alpha = [PanB]/K_M = 1/21$, $\beta = [Mpa]/K_{0.5}$, and L is a conformational equilibrium constant.[35] The dotted line represents the expected curve if Mpa acted as a nonallosteric competitor, based on a simple inhibition model, rate = $V_{max}(S)/(K_{0.5}(1 + (I)/K_i) + (S))$, assuming Mpa and PanB have similar affinities for PafA.[23]

positively affects PanB binding by PafA. As PafA is an allosteric enzyme that binds its target proteins cooperatively,[20] we considered the possibility that the observed activation results from Mpa^{KR} recognition as a substrate by PafA. The mode of substrate recognition by PafA is currently unclear, such that it remains possible that substrate residues other than the pupylation site lysine contribute significantly to PafA binding. However, comparing Mpa^{KR} titrations, as depicted in Figure 3B, with wild type Mpa titrations, suggested this not to be the case. Indeed, while low concentrations of wild type Mpa enhanced PanB pupylation, higher concentrations resulted in decreased PanB pupylation rates (Figure 3C), unlike the effect observed for Mpa^{KR}. The decrease in observed activity reflects competition with PanB for PafA binding, which dominates over the effects of allosteric activation. We conclude that the observed activation of PanB pupylation by Mpa^{KR} does not reflect an enzyme−substrate interaction.

Next, we sought to detect the formation of a Mpa^{KR}-Pup^{E}-PafA ternary complex via *in vitro* pull-down assays. For these assays, we took advantage of the natural adherence of Mpa to agarose beads, a property that we identified during the course of this research. Indeed, Mpa, but not PafA or Pup^{E}, readily binds agarose beads in the buffer used for pupylation and can be eluted at high ionic strength (not shown). Thus, for the pull-down assays, different combinations of Mpa, PafA, and Pup^{E} were mixed with stripped NTA-agarose beads. As PafA is homologous to Dop,[14] similar assays were performed in parallel using Dop instead of PafA. In the assay, elution with buffer containing 500 mM NaCl was carried out following several washing steps, at which point the presence of proteins in the eluate was examined by Western analysis. Dop was not detected in the eluate, regardless of the protein mix used for binding (not shown). By contrast, PafA was detected when Mpa^{KR} was included in the protein mix being tested for binding (Figure 4A). To our surprise, Pup^{E} was expendable for PafA binding by Mpa^{KR}, suggesting a direct interaction between Mpa and PafA.

To determine the affinity of Mpa^{KR} for PafA, we generated a fluorescein-labeled variant of Mpa^{KR} (hereafter, Fl-Mpa^{KR}). *M. smegmatis* Mpa presents three cysteines that can potentially be labeled in a reaction with 5-iodoacetamidofluorescein (5-IAF). We could confirm that the labeled Mpa variant is properly folded, as both Fl-Mpa^{KR} and wild type Mpa hydrolyzed ATP equally well (Figure 4B). Thus, binding assays were carried out in which fluorescence anisotropy was measured at increasing PafA concentrations and a constant low concentration of Fl-Mpa^{KR} (Figure 4C). As the Mpa hexamer is much larger than PafA, a small increase in anisotropy upon PafA binding is expected. Yet, significant anisotropy changes could be detected, allowing us to determine a K_D of 0.3 ± 0.1 μM for the interaction between PafA and Mpa^{KR}. This measurement is consistent with the apparent binding constant measured for activation of PanB pupylation by Mpa^{KR}, as depicted in Figure 3B.

Finally, we wanted to test whether the interaction between PafA and Mpa can be detected *in vivo*. To this end, *M. smegmatis* cell lysates were prepared and co-immunoprecipitation experiments were carried out in which Mpa, the 20S proteasome subcomplex, and Dop were immunoprecipitated using appropriate antibodies. PafA co-immunoprecipitation was subsequently tested by Western analysis. In these experiments, it was important to avoid detection of the heavy chains of the antibodies used for immunoprecipitation, as both PafA and the heavy chains migrate similarly in SDS-PAGE. Therefore, a FLAG-tagged PafA variant was expressed in *M. smegmatis*, thus allowing for immunoprecipitation of Mpa, the 20S, and Dop using rabbit antibodies, followed by Western analysis with mouse anti-FLAG primary antibodies and horseradish peroxidase-conjugated antimouse secondary antibodies. Consistent with the *in vitro* pull-down experiment, PafA could be co-immunoprecipitated with Mpa (Figure 4D). PafA also co-immunoprecipitated with the 20S complex, suggesting that *in vivo*, PafA interacts with fully assembled proteasomes. Our finding that PafA did not co-immunoprecipitate with Dop supports the current understanding that PafA and Dop do not

dx.doi.org/10.1021/bi401017b | *Biochemistry* 2013, 52, 9029−9035

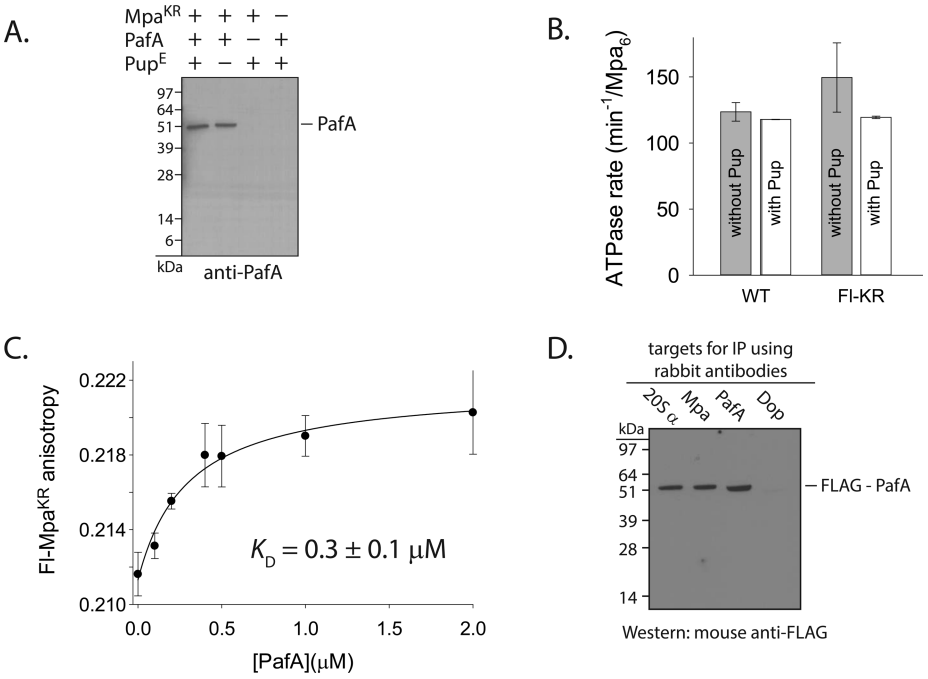

Figure 4. PafA and Mpa^{KR} interact with each other. (A) Combinations of Mpa^{KR} (10 μM hexamer), PafA (10 μM), and Pup^{E} (3 μM), as indicated, were mixed in pupylation buffer containing ATP (1 mM) and applied to NTA-agarose beads. Following washing and elution, Western analysis using anti-PafA antibodies was performed. (B) The rate of ATP hydrolysis by Mpa^{KR} and Fl-Mpa^{KR} (0.3 μM hexamer each) was measured in the absence or presence of Pup^{E} (20 μM). (C) Fl-Mpa^{KR} (25 nM) anisotropy was measured at increasing concentrations of PafA. The curve was generated by fitting the data as described in the legend to Figure 2b. In all graphs, the averages ± SD of three experiments are presented. (D) *M. smegmatis* cells expressing FLAG-PafA were lysed and the 20S α subunit, Mpa, and Dop were immunoprecipitated using specific FLAG-tagged rabbit antibodies. Next, Western analysis using mouse anti-FLAG antibodies was carried out.

interact. This lack of interaction also serves as a negative control, reflecting the specificity of the PafA co-immunoprecipitation seen in our assays.

DISCUSSION

The work presented here indicates that PafA and the micobacterial proteasome can form a complex and that, within this complex, Pup^{E} can interact simultaneously with both PafA and Mpa. Our results do not, however, imply that formation of this complex is essential for either proteasomal degradation or pupylation. Clearly, the proteasome and PafA are active as autonomous units.[17,20,28−30] We can, therefore, ask what purpose would be served by a PafA-proteasome complex? One possible answer is the enhanced degradation of pupylated proteins. In the cell, following pupylation by a proteasome-free PafA, the tagged proteins can undergo either proteasomal degradation or depupylation by Dop. Formation of a PafA-proteasome complex allows pupylation to occur on the proteasome, thus avoiding depupylation by instead channeling substrates from PafA directly to the proteasome. The physiological role of the pupylation system is currently unclear, and as pupylated proteins are not necessarily degraded by the proteasome, it has been surmised that protein pupylation serves regulatory roles.[2,4,15,16] There may exist, however, conditions in which enhanced degradation of pupylated proteins is required. Under these conditions, formation of a PafA-proteasome complex may be the mechanism designed to facilitate degradation. It is also possible that the proteasome degrades untagged proteins, alongside degradation of pupylated proteins, and that PafA, via interaction with the proteasome, shifts the specificity of Mpa toward degradation of pupylated proteins. We find some degree of analogy between this scenario and SspB-mediated degradation of ssrA-tagged proteins by ClpXP. SspB binds both ClpX and the ssrA tag, and, although not essential for degradation of ssrA-tagged proteins, the tethering activity of SspB functions to facilitate degradation of ssrA-tagged proteins.[32,33] For the proteasome, PafA could assume that role SspB plays for ClpXP. Finally, a PafA-proteasome complex may minimize the chances of substrate unfolding and aggregation following pupylation. Pup-tagging could affect proteins in an unpredictable manner. Some proteins would be indifferent to pupylation and maintain their proper folding. For others, pupylation would result in compromised thermal stability and enhanced association with protein aggregates. Substrate channeling from PafA the proteasome could thus prevent potential accumulation of misfolded pupylated proteins in the cytoplasm.

Our data indicate that Pup helix H1 is necessary for efficient binding of Pup by Mpa and by PafA, suggesting that PafA and Mpa binding to this Pup region are mutually exclusive events. Nonetheless, Pup^{E} binding by Mpa does not perturb pupylation or Pup^{E} binding by PafA. This apparent paradox can be resolved, if, for example, the interaction between PafA and Mpa compensates for the loss of a Pup helix H1 interaction with either Mpa or PafA. Clearly, more biochemical and structural studies will be required to adequately address this issue. Likewise, such studies will facilitate elucidation of the interaction interphase between Mpa and PafA, the number of PafA molecules bound by Mpa, and the effect of PafA binding on proteasomal degradation.

Before it was identified as a Pup ligase, PafA was termed "proteasome accessory factor", reflecting that it may recognize a signal on proteins targeted for degradation.[34] This hypothesis was supported by the similar phenotype of *M. tuberculosis paf*

dx.doi.org/10.1021/bi401017b | *Biochemistry* 2013, 52, 9029−9035

and *mpa* mutants.[34] Later, when it was found that PafA functions as a Pup ligase, it was realized that the assigned name does not accurately reflect the biological activity of the protein. Finally, it is ironic that, based on the results of the present study, the original naming assignment for PafA seems justified, now that it has been shown to indeed act as a proteasome accessory factor.

AUTHOR INFORMATION

Corresponding Author

*Tel.: +972-3-6472930; E-mail: gure@bgu.ac.il.

Author Contributions

Nadav Forer and Maayan Korman contributed equally.

Notes

The authors declare no competing financial interest.

ACKNOWLEDGMENTS

We thank Boaz Shaanan and Amir Aharoni (Ben-Gurion University) for helpful advice and fruitful discussions.

REFERENCES

(1) Cerda-Maira, F., and Darwin, K. H. (2009) The Mycobacterium tuberculosis proteasome: more than just a barrel-shaped protease. *Microbes Infect. 11*, 1150−1155.

(2) Barandun, J., Delley, C. L., and Weber-Ban, E. (2013) The pupylation pathway and its role in mycobacteria. *BMC Biol. 10*, 95.

(3) Darwin, K. H., Ehrt, S., Gutierrez-Ramos, J. C., Weich, N., and Nathan, C. F. (2003) The proteasome of Mycobacterium tuberculosis is required for resistance to nitric oxide. *Science 302*, 1963−1966.

(4) Cerda-Maira, F. A., Pearce, M. J., Fuortes, M., Bishai, W. R., Hubbard, S. R., and Darwin, K. H. (2010) Molecular analysis of the prokaryotic ubiquitin-like protein (Pup) conjugation pathway in Mycobacterium tuberculosis. *Mol. Microbiol. 77*, 1123−1135.

(5) Gandotra, S., Lebron, M. B., and Ehrt, S. (2010) The Mycobacterium tuberculosis proteasome active site threonine is essential for persistence yet dispensable for replication and resistance to nitric oxide. *PLoS Pathog. 6*, e1001040.

(6) Groll, M., Ditzel, L., Lowe, J., Stock, D., Bochtler, M., Bartunik, H. D., and Huber, R. (1997) Structure of 20S proteasome from yeast at 2.4 A resolution. *Nature 386*, 463−471.

(7) Hu, G., Lin, G., Wang, M., Dick, L., Xu, R. M., Nathan, C., and Li, H. (2006) Structure of the Mycobacterium tuberculosis proteasome and mechanism of inhibition by a peptidyl boronate. *Mol. Microbiol. 59*, 1417−1428.

(8) Darwin, K. H., Lin, G., Chen, Z., Li, H., and Nathan, C. F. (2005) Characterization of a Mycobacterium tuberculosis proteasomal ATPase homologue. *Mol. Microbiol. 55*, 561−571.

(9) Wang, T., Li, H., Lin, G., Tang, C., Li, D., Nathan, C., Darwin, K. H., and Li, H. (2009) Structural insights on the Mycobacterium tuberculosis proteasomal ATPase Mpa. *Structure 17*, 1377−13785.

(10) Wolf, S., Nagy, I., Lupas, A., Pfeifer, G., Cejka, Z., Müller, S. A., Engel, A., De Mot, R., and Baumeister, W. (1998) Characterization of ARC, a divergent member of the AAA ATPase family from Rhodococcus erythropolis. *J. Mol. Biol. 277*, 13−25.

(11) Pearce, M. J., Mintseris, J., Ferreyra, J., Gygi, S. P., and Darwin, K. H. (2008) Ubiquitin-like protein involved in the proteasome pathway of Mycobacterium tuberculosis. *Science 322*, 1104−1107.

(12) Burns, K. E., Liu, W. T., Boshoff, H. I., Dorrestein, P. C., and Barry, C. E., 3rd (2009) Proteasomal protein degradation in Mycobacteria is dependent upon a prokaryotic ubiquitin-like protein. *J. Biol. Chem. 284*, 3069−3075.

(13) Sutter, M., Damberger, F. F., Imkamp, F., Allain, F. H., and Weber-Ban, E. (2010) Prokaryotic ubiquitin-like protein (Pup) is coupled to substrates via the side chain of its C-terminal glutamate. *J. Am. Chem. Soc. 132*, 5610−5612.

(14) Striebel, F., Imkamp, F., Sutter, M., Steiner, M., Mamedov, A., and Weber-Ban, E. (2009) Bacterial ubiquitin-like modifier Pup is deamidated and conjugated to substrates by distinct but homologous enzymes. *Nat. Struct. Mol. Biol. 16*, 647−651.

(15) Burns, K. E., Cerda-Maira, F. A., Wang, T., Li, H., Bishai, W. R., and Darwin, K. H. (2010) "Depupylation" of prokaryotic ubiquitin-like protein from mycobacterial proteasome substrates. *Mol. Cell 39*, 821−827.

(16) Imkamp, F., Striebel, F., Sutter, M., Ozcelik, D., Zimmermann, N., Sander, P., and Weber-Ban, E. (2010) Dop functions as a depupylase in the prokaryotic ubiquitin-like modification pathway. *EMBO J. 11*, 791−797.

(17) Striebel, F., Hunkeler, M., Summer, H., and Weber-Ban, E. (2010) The mycobacterial Mpa-proteasome unfolds and degrades pupylated substrates by engaging Pup's N-terminus. *EMBO J. 29*, 1262−1271.

(18) Wang, T., Darwin, K. H., and Li, H. (2010) Binding-induced folding of prokaryotic ubiquitin-like protein on the Mycobacterium proteasomal ATPase targets substrates for degradation. *Nat. Struct. Mol. Biol. 7*, 1352−1357.

(19) Barandun, J., Delley, C. L., Ban, N., and Weber-Ban, E. (2013) Crystal structure of the complex between prokaryotic ubiquitin-like protein and its ligase PafA. *J. Am. Chem. 135*, 6794−6797.

(20) Ofer, N., Forer, N., Korman, M., Vishkautzan, M., Khalaila, I., and Gur, E. (2013) Allosteric transitions direct protein tagging by PafA, the prokaryotic ubiquitin-like protein (pup) ligase. *J. Biol. Chem. 288*, 11287−11293.

(21) Norby, J. G. (1988) Coupled assay of Na+,K+-ATPase activity. *Methods Enzymol. 156*, 116−119.

(22) Lindsley, J. E. (2001) Use of a real-time, coupled assay to measure the ATPase activity of DNA topoisomerase II. *Methods Mol. Biol. 95*, 57−64.

(23) Van Kessel, J. C., Marinelli, L. J., and Hatfull, G. F. (2008) Recombineering mycobacteria and their phages. *Nat. Rev. Microbiol. 6*, 851−857.

(24) Festa, R. A., McAllister, F., Pearce, M. J., Mintseris, J., Burns, K. E., Gygi, S. P., and Darwin, K. H. (2010) Prokaryotic ubiquitin-like protein (Pup) proteome of Mycobacterium tuberculosis. *PLoS One 5*, e8589.

(25) Poulsen, C., Akhter, Y., Jeon, A. H., Schmitt-Ulms, G., Meyer, H. E., Stefanski, A., Stühler, K., Wilmanns, M., and Song, Y. H. (2010) Proteome-wide identification of mycobacterial pupylation targets. *Mol. Syst. Biol. 6*, 386.

(26) Watrous, J., Burns, K., Liu, W. T., Patel, A., Hook, V., Bafna, V., Barry, C. E., 3rd, Bark, S., and Dorrestein, P. C. (2010) Expansion of the mycobacterial "PUPylome". *Mol. Biosyst. 6*, 376−385.

(27) Delley, C. L., Striebel, F., Heydenreich, F. M., Özcelik, D., and Weber-Ban, E. (2012) Activity of the mycobacterial proteasomal ATPase Mpa is reversibly regulated by pupylation. *J. Biol. Chem. 287*, 7907−7914.

(28) Burns, K. E., Pearce, M. J., and Darwin, K. H. (2010) Prokaryotic ubiquitin-like protein provides a two-part degron to Mycobacterium proteasome substrates. *J. Bacteriol. 192*, 2933−2935.

(29) Cerda-Maira, F. A., McAllister, F., Bode, N. J., Burns, K. E., Gygi, S. P., and Darwin, K. H. (2011) Reconstitution of the Mycobacterium tuberculosis pupylation pathway in Escherichia coli. *EMBO Rep. 12*, 863−870.

(30) Guth, E., Thommen, M., and Weber-Ban, E. (2011) Mycobacterial ubiquitin-like protein ligase PafA follows a two-step reaction pathway with a phosphorylated pup intermediate. *J. Biol. Chem. 286*, 4412−4419.

(31) Barandun, J., Delley, C. L., and Weber-Ban, E. (2012) The pupylation pathway and its role in mycobacteria. *BMC Biol. 10*, 95.

(32) Levchenko, I., Seidel, M., Sauer, R. T., and Baker, T. A. (2000) A specificity-enhancing factor for the ClpXP degradation machine. *Science 289*, 2354−2356.

(33) Baker, T. A., and Sauer, R. T. (2012) ClpXP, an ATP-powered unfolding and protein-degradation machine. *Biochim. Biophys. Acta 1823*, 15−28.

(34) Darwin, K. H., Ehrt, S., Gutierrez-Ramos, J. C., Weich, N., and Nathan, C. F. (2003) The proteasome of Mycobacterium tuberculosis is required for resistance to nitric oxide. *Science 302*, 1963−1966.
(35) Segel, I. H. (1975) *Enzyme Kinetics: Behavior and Analysis of Rapid Equilibrium and Steady-State Enzyme Systems*, pp 421−461, John Wiley & Sons, Inc., New York.